Influence of Conformational Effects on Spectroscopic Properties of 2-Dimethylamino-9(4′-dimethylamino) phenyl-9-fluorenol[1]

T. Redzimski[2] and J. R. Heldt[2,3]

Absorption and fluorescence spectra of 2-dimethylamino-9(4′-dimethylamino)phenyl-9-fluorenol have been studied in different solvents. The fluorescence spectra at various temperatures show the excitation wavelength dependence. The spectroscopic data are compared with the results of the quantum chemical calculation obtained using PM3 and INDO/S methods. The fluorescence decay curves of the molecule under study can be only satisfactorily fitted by a biexponential function. The steady state and time resolved spectroscopy studies as well as the theoretical calculation confirm that in methylcyclohexane and ethyl acetate solutions always two absorbing and emitting species exist, namely rotamers α and β in the ground and excited states.

KEY WORDS: Fluorene derivatives; rotamers luminescence parameters.

INTRODUCTION

Recently by us [1,2] and by other authors [3–7] several amino derivatives of fluorene and fluorenone have been studied. It has been shown that its fluorescence spectra strongly depend on the type and place of substitution of the amino group at the parent moiety. For amino derivatives the S_1 state deactivates efficiently via the internal conversion mechanism whereas only for 1-dimethylamino substituted compounds via the conformational relaxation mechanism [3]. Also we have shown that 2-dimethylamino or 2-diethylamino fluorenes in protic solvents show the negative solvation effect which causes a significant change (decrease) of the fluorescence quantum yields, Q_F, fluorescence decay time, τ_F, and hipsochromic shift of the fluorescence spectra at room temperature. Nevertheless, the experimental fluorescence decay curves of those compounds are well fitted by a single exponential function.

Because the spectral and photophysical parameters of these derivatives of fluorene are very sensitive to the environment they are widely used as a probe fluorophores to characterize biomimetic systems and biomembranes [8–11]. A particular group of fluorene derivatives are the poly-nitro-9-fluorenes possessing ability to form the charge-transfer complexes. These well known acceptors of π-electrons are widely used to sensitize the photoconductivity of carbazole-containing polymers [12].

It was tempting for us to check how two electron donating substituents, i.e. dimethylamino-$N(CH_3)_2$ and -9(4′-dimethylamino)phenyl functional group substituted at 9 position of fluorenol, affect the photophysical and luminescence parameters of the parent molecule, being dissolved in different solvents at various temperatures. In order to give sufficient presentation, the obtained results were compared with the well known data of fluorene.

Experimental Details

The steady and time resolved spectroscopic measurements of the 2-dimethylamino-9(4′-dimethylamino) phenyl-9-fluorenol (further referred to as **II**) were performed using the same apertures as in [1,2]. Thus we refer to our earlier publications in order to learn about experimental procedures and details.

RESULTS AND DISCUSSION

Steady-State Absorption and Emission Spectra

The absorption spectra of fluorene and its amino derivative **II** in McH and EtOH solution at room temperature are shown in Fig. 1A. The spectra in solvents differ significantly from the well known fluorene spectrum [13]. They are composed of very intense band at $\lambda_{max} = 225$ nm, and two broad bands at $\lambda_{max} = 265$ nm and a very weak one in the 290–370 nm region. Comparing its structure with these of fluorene, distinct similarities can be also recognized. According to the spectrum of fluorene [14] the very strong band in 225–300 nm region contains three transitions: first at 300 nm ^1L_b ($1^1B_2 \leftarrow {}^1A_1$), second, stronger, at 260 nm $^1B_2$ ($2^1B_2 \leftarrow {}^1A_1$), polarized along the long axis of the molecule and third the weak one at 273 nm ^1L_a ($2^1A_2 \leftarrow {}^1A_1$) short axis polarized. As can be seen in Fig. 1A, the introduction of the $-N(CH_3)_2$ group in position 2 of fluorene skeleton perturbs the long axis transitions in agreement with the results of [2,4]. On the other hand, the phenyl group sub-

stituted additionally with another $-N(CH_3)_2$ substituent at position 4′ attached to fluorene in position 9 perturbs the transitions appearing at both axes, i.e. ^1L_b, $^1B_2$ and ^1L_a [14,15]. These suppositions are confirmed by the obtained results of the absorption measurements. As can be seen in Fig. 1A, the derivative of fluorene **II** possesses the absorption band maxima shifted to a longer wavelength, comparing to parent molecule, with deprivation of the vibrational structure, present in fluorene absorption spectrum. The longest absorption band at $\lambda_{max} = 350$ nm, according to [16], can be assigned straightforward as the delocalized charge transfer band arising from the interaction between the dimethylamino donor group and the fluorene ring. This band shows typical features of a charge transfer transition such as a broad and structureless shape. Similar to other amines [4], this band is red shifted with increasing the polarity of the solvent.

Figure 1B displays the fluorescence spectra of **FL** and the compound **II** in non-polar (McH), polar nonprotic (EtAc) and (AcN) and protic (EtOH) solvents at 293 K. The fluorescence spectra of **II** molecule do not show mirror symmetrical shape with the long wavelength absorption band unlike those for fluorene. The half width and shape of fluorescence spectrum of **II** are very sensitive to the solvent polarity. These findings point out that in the S_1 state a great charge transfer process takes place from amino group to the aromatic ring of the parent molecule. This effect is doubled due to presence of the two donor substituents in **II** comparing it to 2-dimethylamino-9-fluorenol [2]. The maximum of fluorescence band is red shifted by about 1600 cm^{-1} according to fluorene spectra
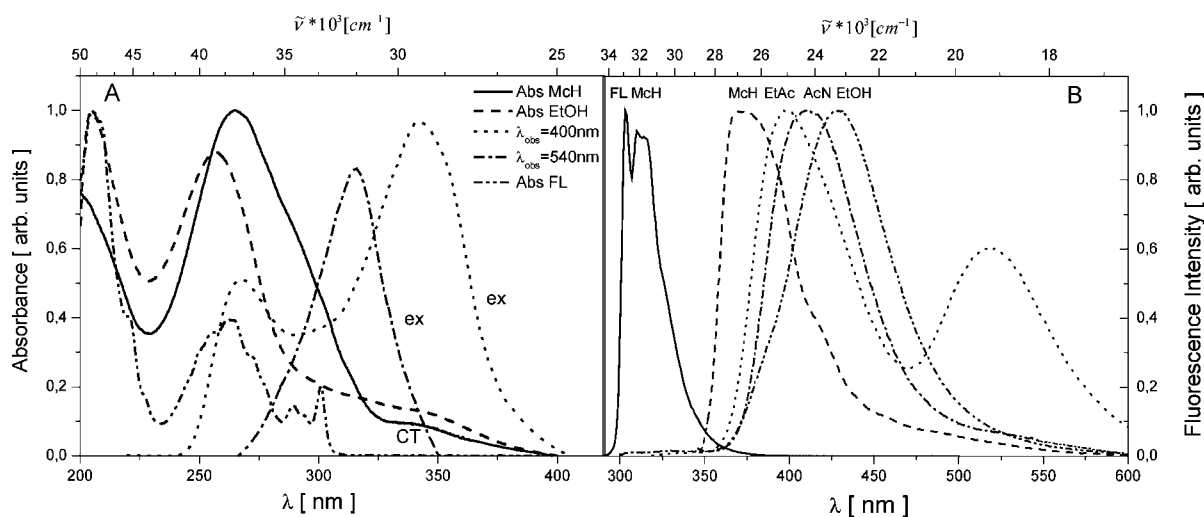

Fig. 1. Absorption spectra of II in McH and EtOH and FL in McH. Excitation spectra of II in EtAc for $\lambda_{obs} = 400$ nm and 540 nm (A). Fluorescence of Fluorene in McH and **II** molecule in McH, EtAc, AcN, EtOH solution (B).

in McH. The batochromic shift of the fluorescence spectrum increases along with increasing polarity of the solvent, which indicates that the lowest excited state S_1 has a π^* nature. Also, it is clearly seen in Fig. 1B that the fluorescence spectrum of **II** in the McH possesses a distinct shoulder at the long wavelength side of the emission band. In EtAc this shoulder appears as the second band. From our previous work [2], concerning the studies of 2-dimethylamino-9-fluorenol and 2-diethylamino-9-fluorenol, it results that dimethyl/diethylamino substituent at position 2 of fluorene does not create a second band (CT band) in the fluorescence spectra. These results are in agreement with the literature findings, showing that the second TICT emission band appears only if the dimethylamino group is substituted at position 1 or 4 of fluorenone and fluorene ring [3]. Since in the molecule under study the 9(4′-dimethylamino)phenyl and —OH group are substituted at 9 position of the fluorene ring the second band ($\lambda_2 = 520$ nm) appearing in some non-polar and weak polar aprotic solvents must have a different reason nature.

It is also worth noticing that in polar protic solvents (EtOH, MeOH) at room temperature, the amino derivatives of fluorene form intramolecular hydrogen bonding [17,18]. As a results, the $\tilde{\nu}_{max}^{FL}$ position of the fluorescence spectra in EtOH ($\varepsilon = 24.5$) is shifted to the longer wavelength, about 1020 cm^{-1}, in comparison to the fluorescence spectra in AcN (even if the letter one has higher static dielectric constant $\varepsilon = 37.5$). It points that **II** forms hydrogen-bonded complexes with alcohol.

Figure 1A shows additionally the fluorescence excitation spectra of **II** in EtAc observed for $\lambda_{obs} = 400$ and 540 nm at room temperature. Their pronounced wavelength dependence, i.e. long wavelength peak maxima at 345 nm and 310 nm indicate the existence of two emitting species responsible for the fluorescence band at $\lambda_1 = 395$ nm and $\lambda_2 = 520$ nm. The absorption and fluorescence spectra measurement performed for different solute concentrations in EtAc [1] show that the ratio of fluorescence intensity bands I_{395}/I_{520} does not depend on the solute concentration. These findings exclude appearance of the solute aggregates in EtAc solution.

In order to confirm the above supposition, the measurement of the fluorescence spectra of **II** has been performed as a function of the solvent temperature and excitation wavelength. Figure 2 shows the fluorescence
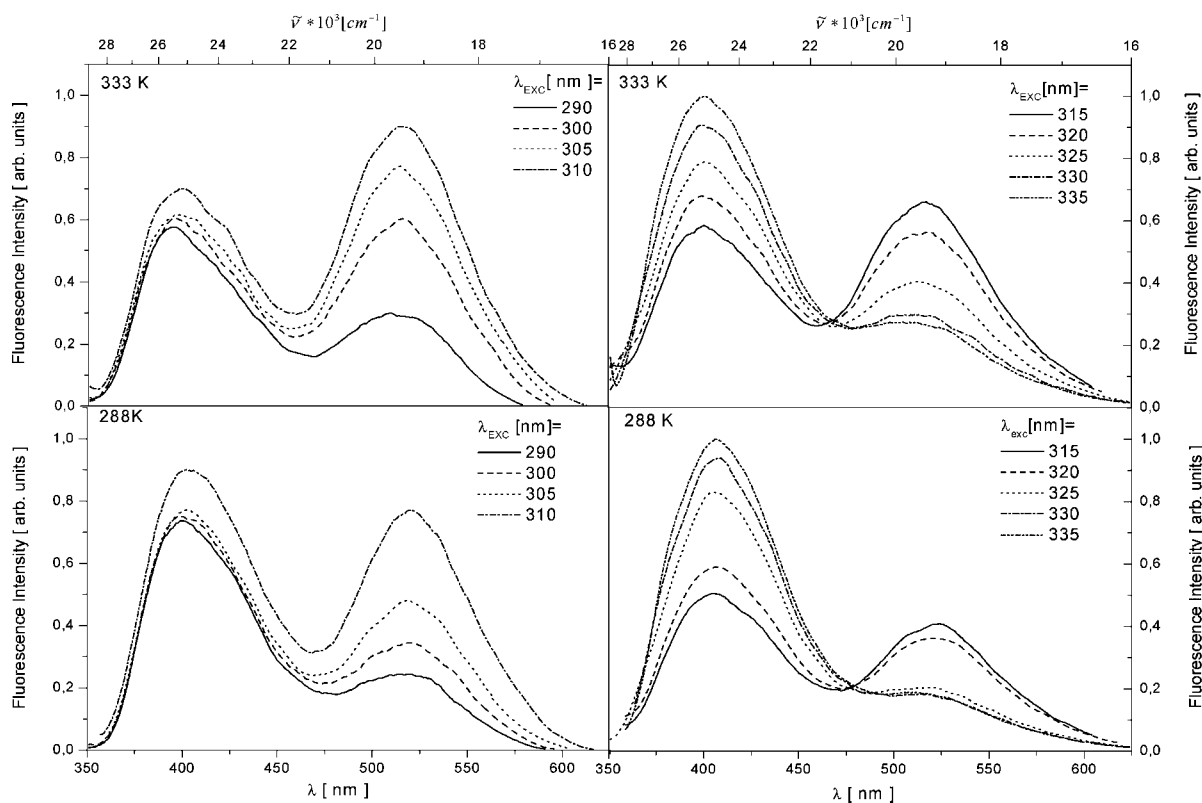

Fig. 2. Fluorescence spectra of **II** at 333 K and 288 K in EtAc at different excitation wavelength.

spectra of **II** molecule obtained for two temperatures, i.e. 288 K and 333 K. The obtained experimental results show that when increasing the temperature of the sample the fluorescence intensity of the short wavelength band, I_1 (350–450 nm) decreases whereas the long wavelength band intensity I_2, (450–600 nm) increases. It is obvious that this intensity change corresponds to a change in the number of emitting species of each kind. It is also worth noticing that the temperature increase leads to the decrease of the fluorescence intensity of the short wavelength band ($\lambda_{max} = 400$ nm) and at the same time an intensity increase of the long wavelength band ($\lambda_{max} = 540$ nm).

Figure 2 shows that the fluorescence intensity of the particular band and its wavelength maxima depends on the excitation wavelength. The executive analysis of these spectra shows that fluorescence intensity ratio I_1/I_2 decreases if the molecule **II** is excited in the region 290–310 nm and increases for excitation within 315–335 nm. These dependence recourses for temperatures between 288–333 K. It clearly indicates that the emitting species in used solutions (EtAc, ThF, McH) consist space inhomogeneous system.

Very interesting information about the nature of complexes formed between **II** and solvent molecules provided luminescence measurements performed at liquid nitrogen temperature. Figure 3 shows the luminescence spectrum (fluorescence and phosphorescence) of **II** and **FL** in McH obtained at 77 K. This spectrum shows that the specific complex between the solvents and the solute molecules is preserved. The λ_{max}^{FL} value in liquid nitrogen equals 24 530 cm^{-1}. It is shifted to a higher wavenumber by about 1200 cm^{-1}, and in comparison with the room temperature spectrum in EtOH it shows a hypsohromic shift. The presence of hydroxy and -9(4′-dimethylamino)phenyl group at position 9 of fluorene, causes the lack of a clear oscillating structure. The energy gap $\Delta E = E(S_1) - E(T_1)$
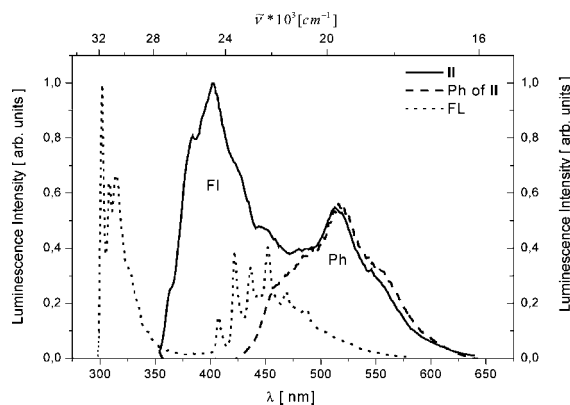
between the S_1 and T_1 states equals 8540 cm^{-1} for **FL** and 4690 cm^{-1} for **II** derivative. The molecule under study (**II**) possesses fluorescence and phosphorescence spectra shifted to the long wavelengths by about 7200 cm^{-1} and 3000 cm^{-1} according to fluorene, respectively. It must be noted that in glassy McH the fluorescence spectrum is only slightly shifted towards higher wavenumber in comparison to its position in EtOH at room temperature. It shows a blurred oscillation structure. Quite long phosphorescence decay time (>1 s) of **II** in McH suggests that the lowest triplet state has $\pi\pi^*$ nature. The emission in both solvents at 77 K is actually a superposition of emissions of the two conformers existing in the room temperature.

Taking into account our earlier spectroscopic data [1,2] and the results discussed above we postulate that **II** molecule possesses the ability to form conformational isomers (rotamers). These rotamers can be created due to the possibility of free rotation of the -9(4′-dimethylamino)phenyl group with reference to the plane of the parent molecule. The photophysical and spectral parameters of particular form of the rotamers depend on their own geometry in the S_1 and S_0 state. The number of rotamers reflects the equilibrium composition of the species in the ground and excited states. This process is possible under the assumption that in S_1 state, the conformational changes of the solute molecule are very fast in comparison to the quite long fluorescence lifetime, τ_F, and that the number of individual kinds of rotamers in the S_1 state is determined by their number in the S_0 state. In order to get additional confirmation of evidence for the existence of rotamers, relevant quantum chemical calculations were performed.

Quantum Chemical Calculations

The standard PM3(MO) method [3,19–21] has been employed for the ground and the excited state geometry optimalization of 2-dimethylamino-9(4′-dimethylamino) phenyl-9-fluorenol. To estimate how the particular substituents —N(CH$_3$)$_2$ and -9(4′-dimethylamino)phenyl influence the spectral parameters, i.e. energy value of S_0 and S_1 states of **II** have been calculated as the function of its dihedral angles.

Figure 4 shows the energy of S_0 and S_1 state of the conformational forms as function of the respective dihedral angels, Θ and ψ. Figure 4A compiles the results when the dimethylamino group in position 2 rotates in respect to the fluorene ring (Scheme A). Figure 4B gives the E_{S_0} and E_{S_1} values obtained when the substituent -9(4′-diemthylamino)phenyl is only turned by ψ and the —N(CH$_3$)$_2$ functional group lies in the plane of

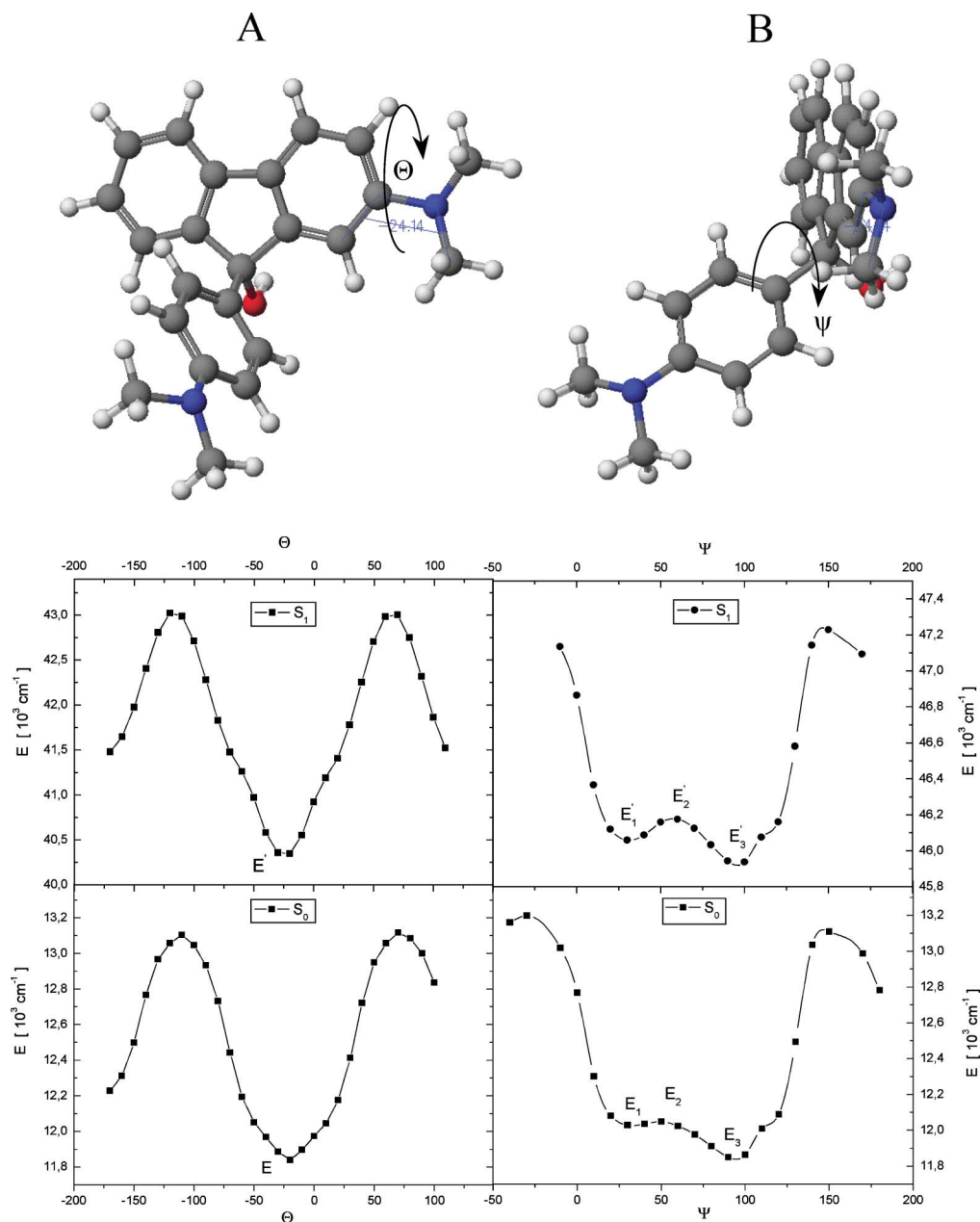**Fig. 3.** Total lumiescence spectra of FL and **II** in McH at 77 K.

Fig. 4. Potential energy as a function of two dihedral angels Θ (A) and ψ (B) for the ground (S_0) and first excited singlet state (S_1) of **II**.

fluorene (Scheme B). The internal energy formation of the conformational forms of the free molecule was evaluated by the structural optimization without any constrains.

The energy values obtained for different dihedral angle Θ show (see Fig. 4A) that the most stable structure for the molecule under study is for $\Theta = 20^0$ for both S_0 and S_1 states. For the case of the ψ angle changes, the obtained energy data imply very interesting and suggestive informa-

tion about spatial structure of **II**. As we can see (Fig. 4B), in the ground and excited state the energy curves posses two minima corresponding to the existence of two α and β stable conformation structures at $\psi = 30$ and 90 degrees. The $\Delta E = E' - E$ and $\Delta E_1 = E_1' - E_1$ difference between the energy curves minima corresponds to the transition in the 225–310 nm region of the absorption spectrum and equals 32 360 cm^{-1} and 29 000 cm^{-1}, respectively.

Table I. Experimental and Theoretical Excitation Energies (cm^{-1}) of Singlet and Triplet States and Its Oscilator Strength (f) of α and β Conformers of Molecule **II**

State	$\psi = 30°$ Calc. [cm^{-1}]	f	$\psi = 90°$ Calc. [cm^{-1}]	f	Exp. Abs. [cm^{-1}]	Exp. Exc. [cm^{-1}]	T_n Calc. [cm^{-1}]	T_n Exp. [cm^{-1}]
1.	—	—	—	—	29 170	29 150	22 607	21270
2.	32 370	0,20	32 270	0,232	—	31 850	25 460	
3.	33 420	0,35	33 670	0,26	33 430	33 840	27 322	
4.	34 080	0,07	34 160	0,15	—	—	30 090	
5.	34 860	0,11	34 660	0,10	—	—	30 826	
6.	39 000	0,56	39 340	0,59	37 640	37 520	32 320	
7.	41 490	0,16	41 040	0,16	—	33 013		
8.	43 430	0,06	43 250	0,02	—	33 640		
9.	44 590	0,02	44 750	0,02	—	33 901		
10.	45 120	0,26	45 270	0,18	—			
11.	49 780	0,51	49 980	0,86	50 400	—		

They are in agreement with the experimental absorption value of the long wave absorption band (310–345 nm) and correspond to the λ_{max} of the fluorescence excitation spectra obtained at $\lambda_{obs} = 400$ nm and $\lambda_{obs} = 540$ nm in EtAc solution. The calculated energy curves indicate that -9(4'-dimethylamino)phenyl substituent is responsible for the existence of conformers which have different emission spectra. These conformers exist in the ground and excited state with a small activation barrier which additionally depends on viscosity of the environment and kind of surrounding molecules.

Additionally, we calculated the energy values of the singlet, S_n, and triplet, T_n, states up to 6 eV and the oscil-

lator strength (f) of $S_0 - S_n$ transitions, using a variant of the INDO/S method of Zerner and Ridley [22–25]. In our calculations, the configuration interaction (CI) was considered by using wavefunction including all electronic states which are generated by singly exciting HOMO and LUMO molecular orbitals. The values of experimental and theoretical E_{S_n}, E_{T_n} and $f(S_0 - S_n)$ data are collected in Table I. The singlet and triplet energy state data were compared with relevant experimental values determined from the absorption, excitation and phosphorescence spectra. Simulated absorption spectra of **II** molecule are in agreement with the experimental ones. Figure 5 shows decompositions into Gaussian curve profiles of the
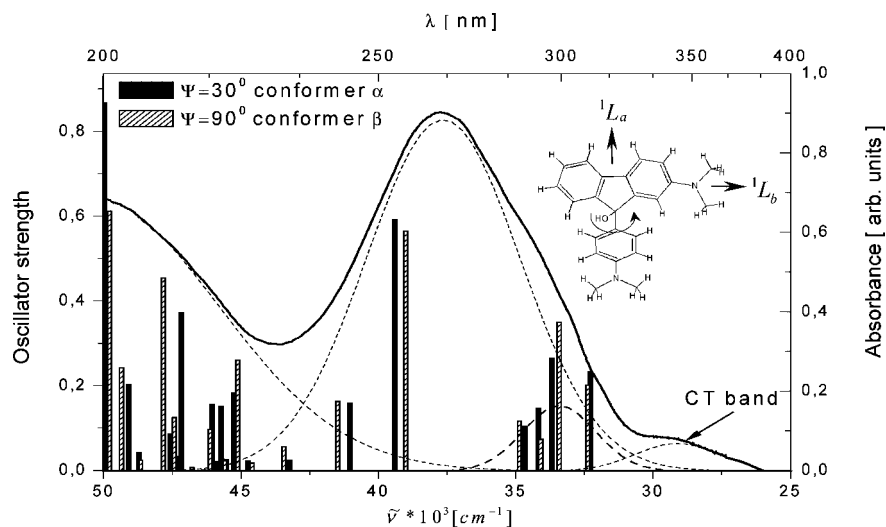

Fig. 5. Normalized UV absorption spectrum of **II** in McH decomposed into Gasuss curve. The black and strip bars represented the vertical excitation energies of α and β conformers, respectively, and its correspoding oscillator strengths as obatined from INDO/S-CI calculation.

absorption spectrum of molecule **II** in McH. This calculations were performed for two different position of -9(4'-diemthylamino)phenyl group according to fluorene plane $\psi = 30$ and 90 degrees. The black vertical bar corresponds to the transition and its oscilator strength of the α conformer and stripe one to the β conformer. The transitions of the β conformer are slightly shifted towards higher energies compared to the α conformer. The fluorene main long axis transitions $1B_2$ (33333 cm^{-1}) and $2B_2$ (38020 cm^{-1}) [14] are present in our calculations for both conformers possesses higher f value in accordance to a parent molecule **FL**. It is caused probably by the donor dimethylamino group at position 2 of parent molecule, disturbing the long axis transition. Analyzing the f value assembled in Table I it follows that the oscillator strength of α conformer differs from that of the β one. Also the data collected in Table I show that the energy values of particular transition are similar for both conformers except their oscillator strength for $S_n \rightarrow S_0$ transition in the region between 35000–30000 cm^{-1}. It can be seen that the absorption spectra of **II** molecule possess a very broad CT band in the region 290–370 nm which does not appear in our calculation. Its existence can be only explained on the basis of its creation by the solution as the results of charge transfer shift of a longwave lying transition [16]. Additionally, for the studied derivative of fluorene main transitions are accompanied by several close lying bands, possessing non-zero oscillator strength, which are not present in fluorene.

Calculated energy value of the triplet state is compared with the experimental value obtained from the phosphorescence spectrum. This value for **II** is quite accurate. It must be noted that the $E(T_2)$ value is smaller than that of the $E(S_1)$ state. This explains the existence of stronger phosphorescence according to it in fluorene.

Analyzing the fluorescence spectra of **II** in EtAc obtained at different temperatures (see Figure 6) it is obvious that the mutual fluorescence intensity changes of I_1^α and I_2^β of both conformers are caused by some internal conformational relaxation processes appearing in the molecule. The observed fluorescence intensity changes of the I_1^α and I_2^β band caused increasing the temperature of the sample clearly indicate that the deactivation of the excited state of **II** is governed by the solvent viscosity and rigidity of the fluorene skeleton. The torsional motion of the —N(CH$_3$)$_2$ and -9(4′-dimethylamino)phenyl substituents are responsible for the conformational relaxation. The release of these torsion vibrations in the molecule under study needs some activation energy. If the conformational relaxations fully describe the radiative deactivation process, e.g., if the inequality $k_F + k_{ISC} \leq k_{CON}$ for both rotamers must be fulfill. Then the deactivation rates, i.e. the radiative decay, k_F, the intersystem crossing rate constant, k_{ISC} and conformational relaxation constant, k_{CON}, are closely correlated to the diffusion motion. According to Alwattar *et al.* [26] the deactivation rate of such folded molecules as **II** must be described by the force volume concept in the diffusion process. In this case, the radiative deactivation rate of **II** is expressed by:

$$\frac{k_F \eta}{T} = A + B \exp[(E_1 - E_2)/RT], \qquad (1)$$

where, E_1 — activation energy of the solution viscosity, E_2 — activation energy of the substituents movment into
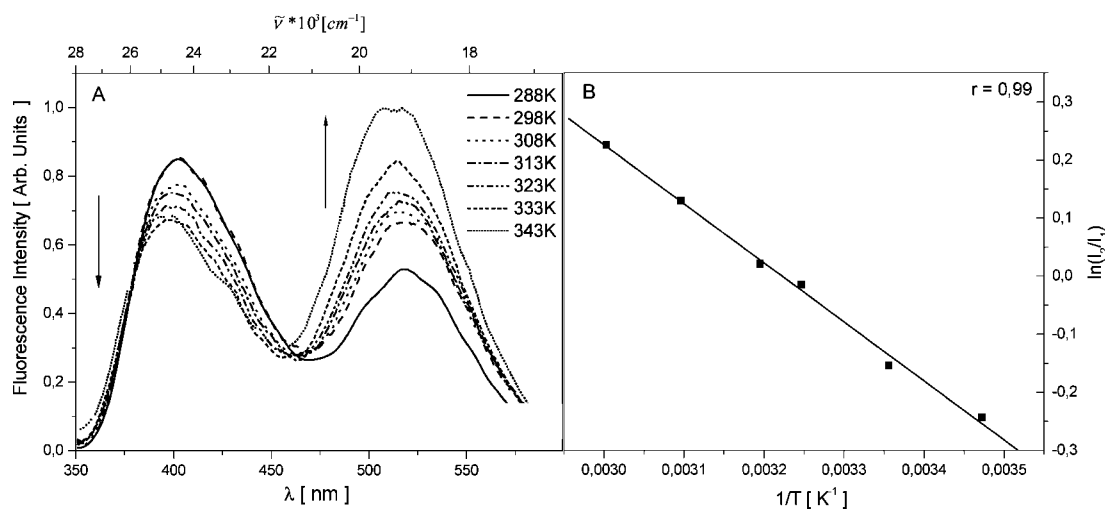

Fig. 6. Fluorescence spectra (A) of **II** in EtAc in different temperature at $\lambda_{exc} = 300$ nm (A) and the Arrhenius plot for the rate on intensity $\ln(I_2^\beta/I_1^\alpha)$ EtAc vs reciprocal of temperature (B).

the free space which is equal to the intramolecular barrier of the torsional vibration of the substituents —N(CH$_3$)$_2$ and -9(4′-dimethylamino)phenyl. Activation energy $E_1 = 632 \text{ cm}^{-1}$ was experimentally determined from the Arrhenius equation $\eta = \eta' \exp(E_1/RT)$ describing the viscosity changes cause by temperature (Here η' is the viscosity at $T = \infty$, R—Rydberg constant).

Due to the lack of relevant experimental set-up, it was difficult for us to obtain the relation between the fluorescence decay times at different temperatures and k_F and, in consequence, the evaluation of the intramolecular activation energy and the rate constant k_{CON}. In spite of that fact, we measured the fluorescence emission at a different temperature (Fig. 6A) at $\lambda_{exc} = 300$ nm. On the basis of Fig. 6A the graph of logarithm of the fluorescence intensity bands ratio I_2^β/I_1^α obtained for various reciprocal temperatures T^{-1} is drawn (see Figure 6B). A good linearity is noted ($r = 0.99$). As it can be seen, the results fulfill the Arrhenius low:

$$\ln\left(\frac{I_2^\beta}{I_1^\alpha}\right) = -\frac{\Delta E}{RT}. \tag{2}$$

Since the intensity ratio I_2^β/I_1^α is directly proportional to the ratio of the deactivation constants, it can be used to determine the intramolecular activation energy E_2. The activation barrier determined from the slope equals to about 820 cm^{-1} and can be identified as the sum of the activation energies $E_1 + E_2$ of the solvent viscosity. From Fig. 4B, the calculated energy differs $\Delta E = E_2' - E_3' \cong E_2 - E_3 \cong 200 \text{ cm}^{-1}$ and, as follows, the potential curve corresponds to the intramolecular activation energy E_2 of the conformational relaxation. This energy is rather small in comparison to E_1(200 cm^{-1} contrary to 632 cm^{-1}) and should not influence drastically the fluorescence decay time. It is also worth noticing that E_2 depends on torsional vibrations of the -9(4′-diemthylamino)phenyl substituent in EtAc solvents.

Time Resolved Spectroscopy

The fluorescence decay time measurements of the molecule under study were taken for McH, ThF and EtOH solutions. Observations were performed for wavelengths corresponding to fluorescence maxima. The excitation wavelength $\lambda_{exc} = 280$ nm corresponds to the region of the strongest band in the absorption spectrum. The τ_F data are compiled in Table II. The fluorescence decays of molecule **II** are well characterized by a double exponential function fitted with a good $\chi^2 \cong 1$ and autocorrelation values (Table II).

Table II. Fluorescence Decay Time of Molecule II in Different Solutions

Solvent	McH		ThF		EtOH	
λ_{obs} [nm]	375	435	400	512	415	490
τ_1[*10^{-9} s]	**1.51**	**1.89**	**1.76**	**1.70**	**1.67**	**1.64**
α_1	12	52	24	31	23	29
τ_2[*10^{-9} s]	**3.41**	**4.30**	**4.39**	**6.66**	**5.92**	**6.6**
α_2	88	48	76	69	77	71
χ^2	*1.10*	*1.08*	*1.09*	*1.26*	*1.11*	*1.09*

We suppose that the two exponential fluorescence decays manifest the presence of rotamers causing inhomogeneousity of the luminescent solution in S$_0$ and S$_1$ states. The absence of a rise time component suggested that the equilibrium between the rotamers α and β is established in the sub-nanosecond time sale as predicted for bianthryl [27]. It is understandable since the activation barrier between the two conformational states is small. The obtained results of fluorescence decay time in McH confirm a dual emission: attributed to the emission from S$_1$ state of α and β conformer. We believe that the noted increase of τ_1 and τ_2 from 4.30 ns to 6.61 ns for the short wavelength band and 3.41–5.92 ns for the long wavelength band is caused by the polarity change and solvation processes of the solvents used. The τ_1 value of the first component in biexponential decay in McH refers to fluorescence, which shows an irregular dependence on the solvents and observation wavelength. In all cases the τ_1 values are shorter than τ_2 (they differ by a factor of about 3). We supposed that **II** molecule in EtOH solution forms a complex between solute and proton donating solvent. Analyzing Table II we can see that the value of τ_1 is comparable for all media used, in opposition to the τ_2, where the noted difference can be ascribed to the hydrogen bond complexes.

CONCLUSION

The detailed data analysis of the steady state and time-resolved measurements as well as the results of quantum chemical calculation can be summarized as follows:

- 2-dimethylamino-9(4′-dimethylamino)phenyl-9-fluorenol shows dual emission in weak polar and medium polar non-protic solvents at different temperatures
- The intensity changes of both fluorescence bands noted by changing the temperature and excitation wavelength, λ_{exc}, confirms the existence of α and β rotamers for the investigated molecule in the

ground and excited state with a small activation energy $E_1 = 200$ cm^{-1} between them.

- The rise of solution temperature results in the decrease of the fluorescence emitted by the α conformer and, at the same time, in the increased intensity contribution by the β conformer.
- The fluorescence decay curves of **II** in three representative solvents can be fitted by two exponential functions only. These findings confirm the assumption that for the molecule under study exist conformational structure and some relaxation process takes place between them.
- The quantum chemical calculation justifies the above hypothesis that molecule **II** in all solvents used constitutes an inhomogeneous system in which two stable rotamers exist.
- The computed energies (INDO/S method) of the S_n and T_n states and their oscillators strength for the respective transitions are in agreement with the experimental data.

ACKNOWLEDGEMENT

REFERENCES

1. J. Heldt, J. R. Heldt, T. Redzimski, H. Diehl, and P. Schultz (2000). *Z. Naturforsch. A.* **55**, 1A.
2. T. Redzimski and J. R. Heldt (2003). *J. Fluoresc.* **13**, 393.
3. Morimoto, L. Biczók, and others (2002). *J. Phys. Chem. A.*
4. S. K. Saha and S. K. Dogra (1998). *J. Mol. Struct.* **470**, 301.
5. Sarkar and S. Chakravorti (1998). *J. Lumin.* **78**, 205
6. R. Manoharan and S. K. Dogra (1987). *Can. J. Chem.* **65,** 2013.
7. R. Manoharan and S. K. Dogra (1988). *Can. J. Chem.* **66**, 2375.
8. H. Shizuka (1985). *Acc. Chem. Res.* **18**, 141.
9. M. Swaminathan and S. K. Dogra (1983). *J. Am. Chem. Soc.* **105**, 6223.
10. J. K. Dey and S. K. Dogra (1990). *Chem. Phys.* **143**, 97.
11. J. R. Lakowicz (1983). *Principles of Fluorescence Spectroscopy*, Plenum, New York, Chapter 3.
12. T. K. Mukherjee and L. A. Levasseur (1965). *J. Org. Chem.* **30**, 644.
13. B. Berlman (1971). *Handbook of Fluorescence Spectra of Aromatic Molecules*, Academic Press, New york; B. Berlman (1970). *J. Phys. Chem.* **74**, 3085.
14. A. Bree and R. Zwarich (1969). *J. Chem. Phys.* **51**, 903M.
15. P. Swiderek, M. Michaud, and others (1991). *Chem. Phys. Lett* **187**, 583.
16. M. Maus, W. Rettig, and others (1998). *Chem. Phys. Lett* **292**, 115.
17. L. Skulski (1968). In L. Sobczyk (Ed.), *Wigzania Wodorowe*, PWN Warsaw (in polish).
18. J. Herbrich and J. Waluk (1994). *Chem. Phys.* **188**, 247.
19. M. Brozis, J. R. Heldt, and J. Heldt (2001). *Z. Naturforsch. A* **56**, 841.
20. G. G. Surpateanu, G. Vergoten, and G. Surpateanu (2001). *J. Mol. Struct.* **559**, 263.
21. J. Zhao (2002). *Phys. Lett. Chem.* **351**, 481.
22. J. Ridley and M. A. Zerner (1973). *Theoret. Chim. Acta* **32** , 111.
23. P. Ilich and F. G. Prendergast (1989). *J. Phys. Chem.* **93**, 4441.
24. I. G. Hill, A. Kahn, and others (2000). *Chem. Phys. Lett.* **317**, 444.
25. N. Nakayama and U. Nagashima (2003). *J. Mol. Struct.* **636**, 39.
26. J. B. Birks (1973). *Organic Molecular Photophysics*, London (Chapter 8).
27. M. Mac, P. Kwiatkowski, and U. Pischel (2002). *Chem. Phys. Lett.* **357**, 440.